Gas Permeation Performance of Cellulose Hollow Fiber Membranes Made from the Cellulose/N-Methylmorpholine-N-Oxide/H_2O System

Xingming Jie, Yiming Cao, Bin Lin, Quan Yuan

Laboratory of Environmental Engineering, Dalian Institute of Chemical Physics, Chinese Academy of Sciences, Dalian, China

Received 22 October 2002; accepted 30 June 2003

ABSTRACT: Cellulose hollow fiber membranes (CHFM) were prepared using a spinning solution containing N-methylmorpholine-N-oxide as solvent and water as a nonsolvent additive. Water was also used as both the internal and external coagulant. It was demonstrated that the phase separation mechanism of this system was delayed demixing. The CHFM was revealed to be homogeneously dense structure after desiccation. The gas permeation properties of CO_2, N_2, CH_4, and H_2 through CHFM were investigated as a function of membrane water content and operation pressure. The water content of CHFM had crucial influence on gas permeation performance, and the permeation rates of all gases increased sharply with the increase of membrane water content. The permeation rate of CO_2 increased with the increase of operation pressure, which has no significant effect on N_2, H_2, and CH_4. At the end of this article a detailed comparison of gas permeation performance and mechanism between the CHFM and cellulose acetate flat membrane was given. © 2003 Wiley Periodicals, Inc. J Appl Polym Sci 91: 1873–1880, 2004

Key words: cellulose; hollow fiber membrane; N-methylmorpholine-N-oxide; phase separation; carbon dioxide

INTRODUCTION

The emission of CO_2 and SO_2 resulting from the combustion of fossil fuels such as coal, petroleum, and natural gas is the main cause of acid rain and global warming.[1] During the United Nation Conference on Environment and Development in 1992, strict standards had been established to reduce the emission of greenhouse gases such as CO_2 and SO_2. Removal of CO_2 and H_2S from natural gas is one of the urgent research tasks.[2] Cellulose acetate (CA) membrane is traditionally applied to remove CO_2 from natural gas. Although with an ideal separation factor α (CO_2/CH_4) as high as 30, the CO_2 permeability coefficient (P_{CO2}) is only 5.0 barrer [1 barrer$=10^{-10}$cm^3(STP) cm/(cm^2 s cmHg)], which cannot meet the practical demands. In addition, CA membrane is not good for acid gases separation because of its poor ability to endure acid, alkali, and organic solvents.[3,4] The limitations of cellulose acetate membrane urge the scientists to move their eyes on cellulose, one of the natural polymers.

Cellulose is one of the most abundant resources in the world that can be generated as much as billion tons annually by plants through photosynthesis.[5] Figure 1 is the chemical structure of cellulose, $(C_6H_{10}O_5)_n$, in which n is the polymerization degree of cellulose. There are three active hydroxyls in each repeating unit of cellulose molecule that have strong ability to absorb water molecules and make cellulose highly hydrophilic. Traditionally, cellulose is regenerated or modified by chemical process, in which cellulose degradation will take place and cause an irreversible debasement of its ability to endure severe acid, alkali, and organic solvents, as well as serious environmental problems.[6] Presently, a new cellulose solvent N-methylmorpholine-N-oxide (NMMO) is attracting scientists' attention.[7–9] Through its oxygen atom, which links with the nitrogen atom, NMMO can open the intrinsic hydrogen bonding between cellulose molecules and form new hydrogen bonding with them. In this way cellulose is dissolved by NMMO.[10] Figure 2 shows the dissolution mechanism. The dissolution of cellulose in NMMO is purely physical process without any chemical reaction. It is totally different from the traditional processes that are always being accompanied with chemical reactions. Thus the natural characteristics of cellulose, such as the biocompatibility, are maintained.

Wu et al. demonstrated that cellulose is a promising membrane material for CO_2 removing and recycling.[11] They found that at room temperature, the wet cellulose flat membranes had a P_{CO_2} of 120 barrer at room

Correspondence to: Yiming Cao (ymcao@dicp.ac.cn).

Contract grant sponsor: Chinese Academy of Sciences; contract grant number: DICP R200201.

Journal of Applied Polymer Science, Vol. 91, 1873–1880 (2004)

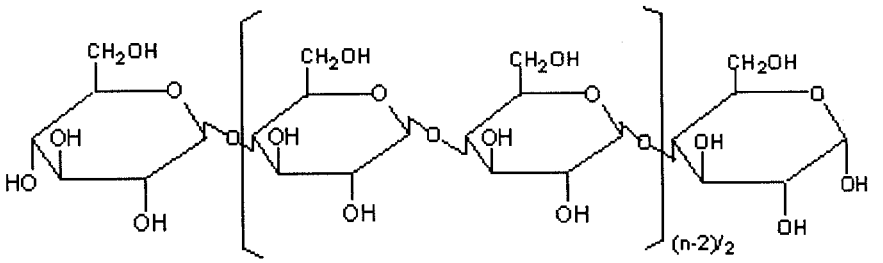

Figure 1 Chemical structure of cellulose.

temperature with pretty high ideal separation factors over N_2, CH_4, and H_2.

Compared with CA, cellulose is more suitable to be the membrane material for the removing and recycling of acid gases (especially CO_2) because of its excellent CO_2 separation performance and superability to endure severe environments. However, there are few reports concerned with the preparation and gas permeation performance of cellulose hollow fiber membranes made from the cellulose/NMMO/H_2O system. In this work, using NMMO as solvent, water as internal and external coagulant, cellulose hollow fiber membranes were prepared by immersion-precipitation and wet spinning. The phase separation mechanism of this system was discussed. The influences of membrane water content and operation pressure on the gas permeation performance of cellulose hollow fiber membranes (CHFM) were investigated. The gas permeation performance and mechanism of the CHFM was compared with CA flat membrane.

EXPERIMENTAL

Materials

Wood cellulose and NMMO · H_2O were purchased from U.S. Sigma Company. The polymerization degree of cellulose was about 1000, with an α-cellulose content larger than 99%. NMMO · H_2O (with water content of 13.3%), which is in the form of white crystal, with a melting point of 72°C, was selected as the solvent.

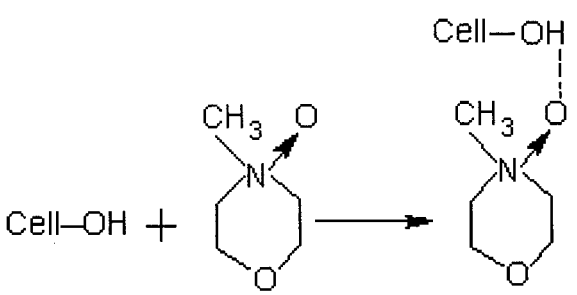

Figure 2 Mechanism of cellulose dissolved by NMMO.

Membrane preparation

A certain amount of cellulose and NMMO°H_2O was mixed at 80°C, with the addition of 0.5 wt % *n*-propylgallate as an antioxidant to avoid oxidation of cellulose during the dissolving process. After being dissolved completely with nitrogen protection and bubble-eliminated under vacuum, the polymer solution containing 10 wt % of cellulose was put into a spinning container that was also kept at 80°C. With dry N_2 as the spinning driving force, the nascent fibers were formed through the spinneret (inner/outer diameter: 0.7/1.4 mm). Once they were immersed in the coagulation water bath at room temperature, coagulation and solidification occurred to form the CHFM. Figure 3 illustrates the spinning process for CHFM. The spinning rate was controlled by N_2 pressure. The bore fluid was water, kept at a flux of 0.6 mL/min with a syringe pump. The CHFM was rinsed with flowing tap water for at least 24 h to remove the remaining solvent.

Membrane desiccation

The wet CHFM was naturally dried in air with a relative humidity of 50% at 25°C. We defined the CHFM that was dried under this environment to be a

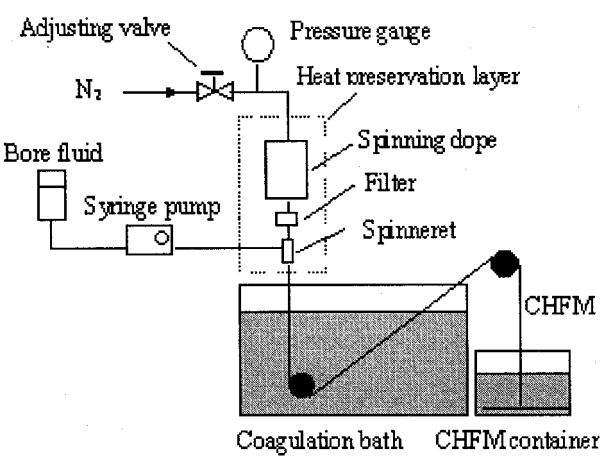

Figure 3 Spinning process for CHFM.

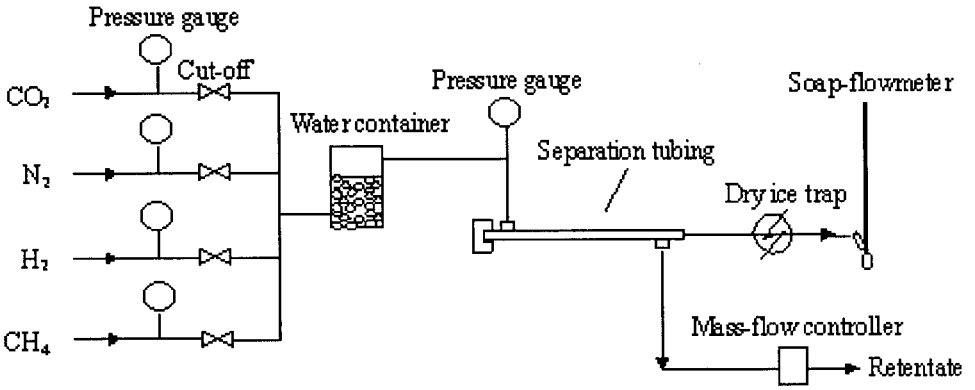

Figure 4 Gas permeation test system for CHFM.

dry CHFM. After desiccation, both the length and diameter of CHFM reduced to about half of its original size, and the dry CHFM had an outer diameter of 0.72 mm and an inner diameter of 0.42 mm. The water content of CHFM has strong influence on its gas permeation performance. So it is necessary to define the water content of CHFM as

$$W_{\mathrm{CHFM}} = \frac{W_W - W_D}{W_D} \times 100\% \quad (1)$$

where W_{CHFM} is the water content of CHFM, W_D is the weight of dry CHFM, and W_W is the wet weight of the CHFM. What should be mentioned is that there is no extra water in the outer and inner surface of wet CHFM, and most of water molecules in CHFM are linking with neighboring cellulose molecules in a state of hydrogen bonding.

Membrane morphology

The cross-sectional structure of the CHFM was examined with an XL-30 scanning electron microscope (SEM) of Philips Company. The samples were freeze-fractured in liquid nitrogen, followed by coating with gold in a sputtering device. The treated samples were placed in the SEM to reveal the membrane.

X-ray diffraction measurement

The X-ray diffraction measurement was carried out, using Ni-filtered and graphite- monochromated CuKα radiation at room temperature, by a Rigaku D/MAX diffractometer. The diffraction profiles were obtained in para focus mode at 40 kV and 100 mA, with a scanning rate of 1.2° per minute. Cellulose powder, cellulose flat membranes, and hollow fiber membranes that were prepared from the same cellulose solution were tested. From the X-ray diffractograms, the degrees of crystallinity were determined using a widely used method.[12]

Gas permeation measurement system

Five fibers of 200 mm in length were encased in a stainless steel tube and arranged in a shell and tube configuration. Both ends of the fibers were potted with an epoxy resin and one end was sealed. CO_2, N_2, CH_4, and H_2 were used respectively as the feeding gas and the permeation path was from the shell side to the bore side. The permeation rate (P/l) is defined by

$$P/l = \frac{p_p V_p}{RT} \frac{V_m}{At(P_r - P_p)} \quad (2)$$

where p_p is the pressure of permeant side (cmHg), p_r is the pressure of retentate side (cmHg), V_P is the volume of permeant gas during the test time (cm^3), V_m is the molar volume for the gas under standard conditions [cm^3(STP) mol^{-1}], t is the test time (s), A is the effective membrane area (cm^2), l is the membrane thickness (cm), R is the gas constant (J mol^{-1} K^{-1}), and T is test temperature (K).

Ideal separation factor of the gases i and j is defined as the ratio of $(P/l)_i$ and $(P/l)_j$ by

$$\alpha(i/j) = (P/l)_i/(P/l)_j \quad (3)$$

Figure 4 shows the gas permeation test system used in the experiments. At room temperature, the feeding gas was pressed into the stainless steel separation tubing through a water container, which could increase the relative humidity of the gas. Then the wet feeding gas permeated from the shell side to the bore side. The wet feeding gas flux was controlled by a mass-flow controller and released to atmosphere from the other end of the separation tubing. The water vapor in the permeant gas was removed by a dry ice-trap and the flux of the permeant gas was measured using a soap flowmeter.

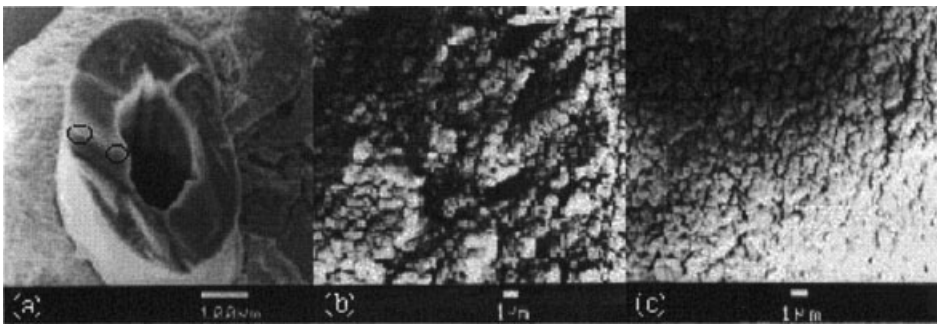

Figure 5 SEM graphs of dry CHFM: (a) cross section, (b) outer part of cross section, and (c) inner part of cross section.

RESULTS AND DISCUSSION

Phase separation of CHFM

Since Loeb and Sourirajan produced the first high-flux desalination CA membrane in 1960, the immersion-precipitation technique has become one of the most popular methods in membrane preparation.[13] During the membrane formation process, once the nascent fiber is immersed into a coagulation bath, an exchange between the solvent and nonsolvent will occur. This causes a liquid–liquid demixing and the homogeneous solution is separated into two parts, one of which is a polymer-rich phase and the other a polymer-lean phase. Following coagulation and solidification in the coagulant bath, the polymer-rich phase forms the membrane structure, while the polymer-lean phase forms the pores. It is a kinetic process and the membrane morphology is determined by the process parameters. Reuvers defined two different mechanisms, instantaneous and delayed demixing, for phase separation of ternary systems by immersion-precipitation.[14,15] Instantaneous demixing occurs when phase separation begins immediately after the immersion (always <1 s), while the delayed demixing takes place if the precipitation path does not cross the binodal for a measurable period of time after contacting with the nonsolvent bath (always >1 s). Membranes formed from instantaneous demixing have a porous top layer and are used in microfiltration and ultrafiltration processes. Membranes formed by delayed demixing have a dense skin and are used in gas separation, pervaporation, and reverse osmosis.

In this article, water was adopted as the coagulant to prepare the CHFM. After the polymer solution was pressed through the spinneret, the nascent fiber was formed and entered into the coagulation bath. At the beginning, the exchange between the solvent (NMMO) and the nonsolvent (water) was so slow that we could not directly observe the phenomenon that the solvent was separated out of the CHFM. When the nascent fiber reached the bottom of the coagulation bath (within about 15 s), an obvious solvent separating-out phenomenon could be seen. This is because there is strong hydrogen bonding between the solvent NMMO and the polymer cellulose, which makes it difficult for the nonsolvent water to replace the solvent NMMO in CHFM quickly. Therefore, the phase separation mechanism of this system should be the delayed demixing, by which the CHFM is prepared with a homogeneous structure. After desiccation the CHFM will have a sharp size reduction and its structure will become very dense. This is because that the water in the wet CHFM took up a large volume of space and the water evaporated from the wet CHFM during desiccation, which provided the neighboring cellulose molecules the chance to join each other and form new hydrogen bonding. This irreversible size reduction will lead to a dense structure for the dry CHFM. Figure 5 is the morphology of dry CHFM. It is obvious that the dry CHFM had a dense structure, and from the picture with high magnification it can be seen that the dry CHFM was composed of many tiny cellulose crystals that are congesting together.

Influence of water content on the gas permeation performance of CHFM

In this work, the influence of water content on the gas permeation performance of the CHFM had been studied. Because of its dense structure, the dry CHFM had very low permeation rates for CO_2, CH_4, and N_2 that were difficult to be determined. When the dry CHFM absorbs some water, the water molecules will depart the neighboring cellulose molecules and form new "water–cellulose" hydrogen bonding instead of the original "cellulose–cellulose" type. In such a way water in the membrane provides a path for the gases to permeate through the CHFM. In other words, the gases are permeating through the water in CHFM and this causes the gas permeation performance of CHFM to greatly improve. Figure 6 shows the effect of water content on the gas permeation rate. Except the all-following dissolution-diffusion mechanism, the water in wet CHFM had an additional facilitating effect on CO_2 permeation compared to other gases. The water plays a carrier role for CO_2 to permeate through wet

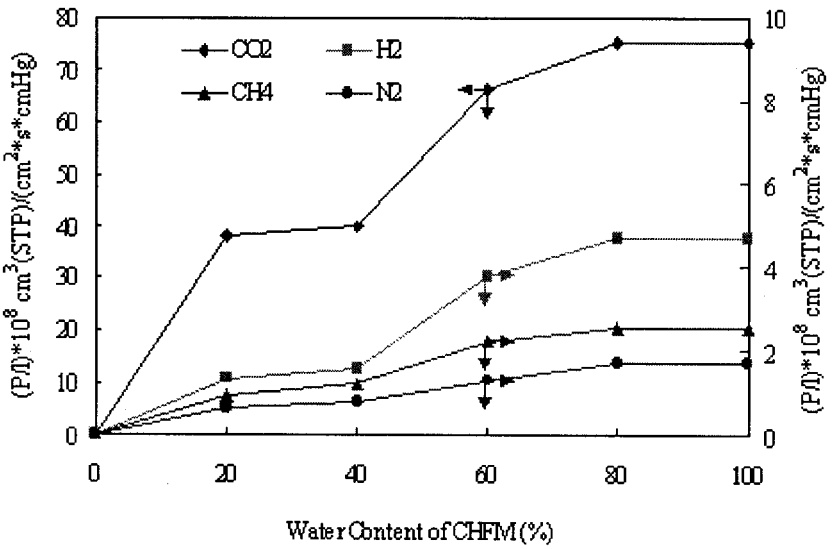

Figure 6 Influence of water content on the gas permeation rates of wet CHFM.

CHFM similar to the facilitated liquid membrane for CO_2 separation. This facilitating effect was realized through a reversible chemical reaction between CO_2 and water: $CO_2+2H_2O \Leftrightarrow HCO_3^- + H_3O^+$. Therefore, the wet CHFM had a much higher permeation rate for CO_2 than other gases. At 25°C and 0.5 MPa, when the water content of CHFM was increased from 20 to 80%, the permeation rates of CO_2, N_2,CH_4, and H_2 all increased, especially in the range from 40 to 60%. When the water content of CHFM was increased to its saturation value (about 80%), $(P/l)_{CO_2}$ reached a maximum value of 75×10^{-8} $cm^3(STP)/(cm^2\ s\ cmHg)$, with ideal separation factors of 45 for N_2, 30 over CH_4, and 16 over H_2. Figure 7 shows the effect of water content on the gas separation factors of wet CHFM. It is demonstrated that with the decrease of water content in membrane, the separation factors increased.

What should be mentioned additionally is that under the same test conditions, gas permeability coefficients of the CHFM prepared in this article are smaller while the separation factor is higher than that of the cellulose flat membrane.[11] For example, P_{CO_2} of the water saturated CHFM was 112.5 barrer (from Table I), which was less than 120 barrer of the wet cellulose flat membrane. The separation factor α (CO_2/H_2) is 16, which is a little higher than 15 of the flat cellulose membrane. This can be explained from the fact that the CHFM, which had been pressed through the spinneret during the formation process, had a more orderly molecular orientation and higher degree of crys-

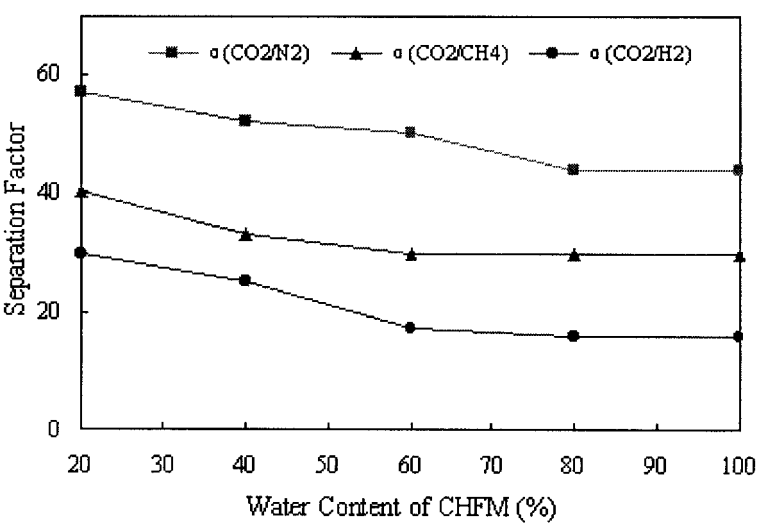

Figure 7 Influence of water content on the gas separation factors of wet CHFM.

TABLE I
Comparison Between the Gas Permeability of CAFM[a] and CHFM

Membrane type	Temp. (°C)	Permeability coefficients (barrer)				Ideal separation factors		
		CO_2	N_2	CH_4	H_2	CO_2/N_2	CO_2/CH_4	CO_2/H_2
Dry CAFM	25	5.0	0.23	0.14	8.4	22	35	0.60
Dry CHFM	25	[—]	[—]	[—]	[—]			
Wet CHFM[b]	25	112.5	2.55	3.83	7.07	45	30	16

[a] Cellulose acetate flat membrane
[b] Wet CHFM (saturation value, see Fig. 6 and Fig. 7); [—]: Too little to be determined.

tallinity than the cellulose flat membrane. This can be proved from the X-ray diffractograms (see Fig. 8). It is shown that the cellulose powder has a degree of crystallinity about 72%, and the CHFM has a value of 63%, which is higher than the cellulose flat membrane prepared from the same cellulose solution, whose degree of crystallinity is 57%.

Influence of operation pressure on the gas permeation performance of CHFM

Influence of pressure on the gas permeation performance of CHFM has also been investigated, and the results are shown in Figures 9 and 10. At 25°C, keeping a wet feeding gas flux of 60 mL/min at 0.4–0.8 MPa, the permeation rates of N_2, H_2, and CH_4 all increased slowly while the permeation rate of CO_2 had a significant increase with the increase of operation pressure. This is because with the increase of the operation pressure, the solubility of water in CHFM also increases, and as we know the water in the CHFM can supply a path for gases to permeate through the membrane. This is because of the additional facilitating effect of water, which made the ideal separation factors of CO_2 over N_2, H_2, and CH_4 also increase with the operation pressure. $(P/l)_{CO_2}$ could reach 44×10^{-8}cm^3(STP)/(cm^2 s cmHg) under 0.5 MPa, which is corresponded to a water content of about 40% in Figure 6.

Comparison between the gas permeability of CHFM with CA flat membrane[3]

The CHFM prepared in this work had a dense structure. The wall thickness of CHFM was determined

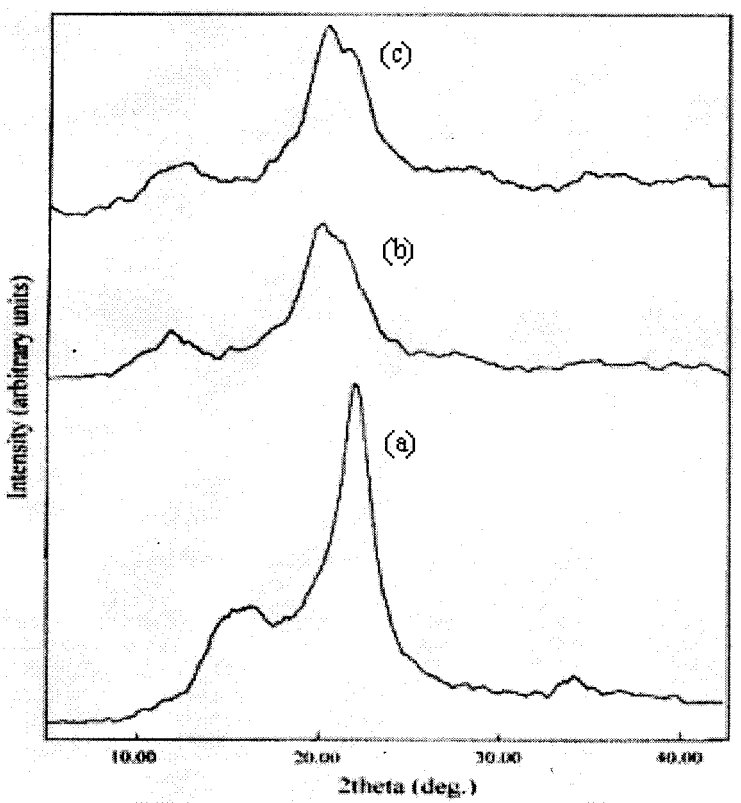

Figure 8 X-ray diffractograms of (a) cellulose powder, (b) cellulose flat membrane, and (c) cellulose hollow fiber membrane.

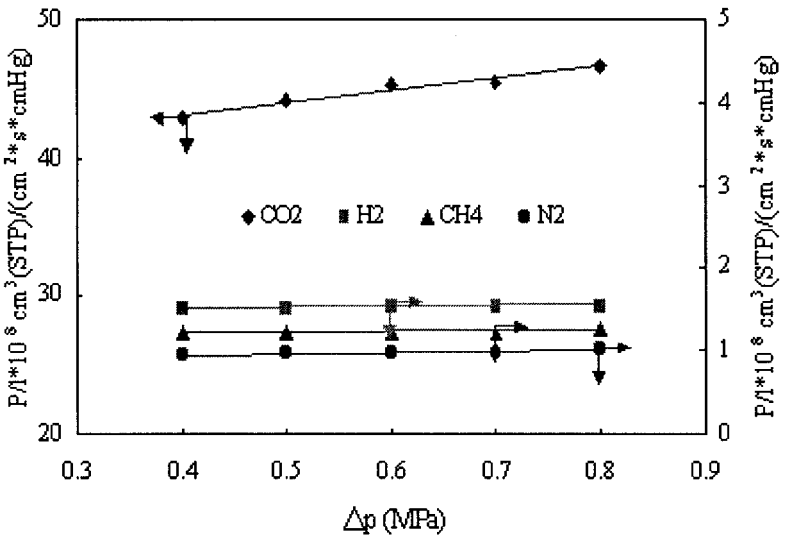

Figure 9 Influence of operation pressure on the gas permeation rates of wet CHFM.

from the SEM pictures, which was the gas permeation resistance layer. By multiplying the thickness by the gas permeation rate of the CHFM, the gas permeability coefficient of CHFM was obtained.

Table I lists the gas permeability coefficients of the CA flat membrane and the CHFM prepared in this article. As we can see, the P_{CO_2} of the CA flat membrane is only 5.0 barrer, which is far less than that of the wet CHFM, which is 112.5 barrer. The permeability coefficient of other gases such as N_2 and CH_4 are much smaller. The P_{H_2} of the CA flat membrane is a little higher than that of the wet CHFM.

After its hydroxyl groups (OH) are substituted by acetyl groups ($OCOCH_3$), cellulose is chemically modified to cellulose acetate. The bulky nature of the acetyl groups reduces the efficiency of chain packing, which also reduces the amount of intermolecular and innermolecular hydrogen bonding and leads to an increase in chain flexibility and mobility. All these give cellulose acetate a totally different structure from cellulose. Compared with cellulose, the structure of CA is much looser because of its few hydrogen bondings between neighboring molecules. Gases permeate through the CA membrane by its molecular chain mobility, which is different from the permeation mechanism of wet CHFM. This is why the dry CA membranes have better gas permeation performance than the dry CHFM. Since the molecular volume of hydrogen is the smallest, H_2 permeate through the CA flat membrane with the highest permeability coefficient.

Because of its strong innermolecular and intermolecular hydrogen bonding, cellulose has much higher

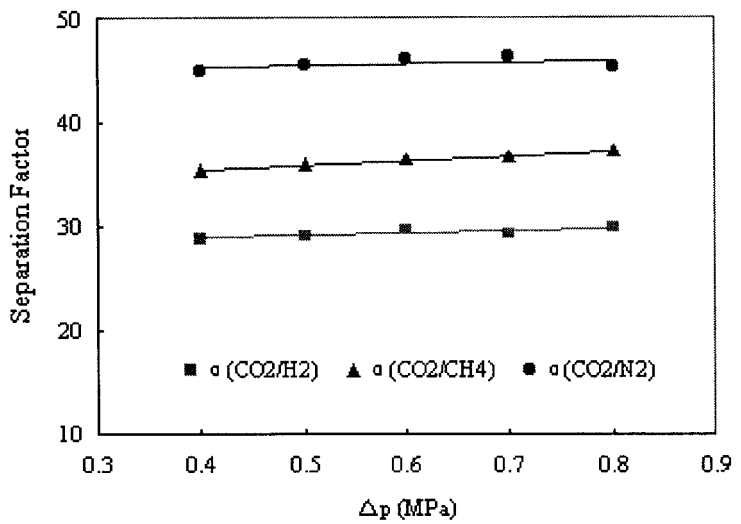

Figure 10 Influence of operation pressure on the gas separation factors of wet CHFM.

chain packing density and higher degree of crystallinity than the CA flat membrane, which causes the dry CHFM to be very difficult for gases to permeate. Only after the dry CHFM has absorbed some water can its strong hydrogen bonding be broken up to result in good gas permeation performance. Especially, because of the great dissolution and diffusion coefficient difference in water between CO_2 and H_2, the $\alpha(CO_2/H_2)$ of wet CHFM can be as high as 16, which means that CO_2 permeates faster than H_2 in wet CHFM, which is absolutely different from the CA flat membrane.

CONCLUSION

Using NMMO as the solvent and water as both the inner and outer coagulant, CHFM was prepared by the techniques of immersion-precipitation and wet spinning. The phase separation mechanism of this system is delayed demixing. After desiccation the dry CHFM has a homogeneously dense structure.

Similar to the cellulose flat membrane, water in wet CHFM supplies permeation paths for gases, and the water content of cellulose membrane has crucial influence on its gas permeation performance. What should be noted is that water in wet CHFM has an additional facilitating effect on CO_2. Gas permeation through the wet CHFM follows the dissolution-diffusion mechanism while gas permeation through the CA membrane is by molecular chain mobility. This causes CO_2 to permeate faster than H_2 in wet CHFM, which is completely opposite from CA flat membrane.

The influence of water content and operation pressure on the gas permeation performance of CHFM has also been studied. At 25°C, keeping a wet feed gas flux of 60 mL/min and at the pressure range of 0.4–0.8 MPa, the permeation rates of N_2, H_2, and CH_4 increased slowly with the pressure, among which the permeation rate of CO_2 had a more obvious increase. At 25°C and 0.5 MPa, when the water content of CHFM was increased to its saturation value (about 80%), $(P/l)_{CO_2}$ reached a maximum value of 75×10^{-8} $cm^3(STP)/(cm^2\ s\ cmHg)$, with ideal separation factors of 45 for N_2, 30 over CH_4, and 16 over H_2. In conclusion, the CHFM prepared has a promising application potential in the field of CO_2 removing and recycling.

References

1. Susumu, N.; Hiroshi, T. Gas Separation and Purification 1994, 8, 107.
2. Bhide, B. D.; Voskericyan, A.; Stern, S. J Membr Sci 1998, 140, 27.
3. Puleo, A. C.; Paul, D. R. J Membr Sci 1989, 47, 301.
4. Hao, J.; Wang, S. Gao Fen Zi Xue Bao 1997, 5, 559.
5. Gao, J.; Tang, L. Cellulose Science; Science Publishing Company: Beijing, 1999.
6. Massimo, B.; Giovanna, F.; Mariastella, S.; Antonino, L. J Appl Polym Sci 2002, 83, 38.
7. Bang Y. H.; Lee, S.; Park, J. B.; Cho, H. H. J Appl Polym Sci 1999, 73, 2681.
8. Yoshihiko, A.; Akira, M. J Appl Polym Sci 2002, 84, 2302.
9. Lewandowski, Z. J Appl Polym Sci 2002, 83, 2762.
10. Maia, E.; Peguy, A.; Perez, S. Acta Cryst 1981, B37, 1858.
11. Wu, J.; Yuan, Q. Membr Sci 2002, 204, 185.
12. Rabek, J. F. Experimental Methods in Polymer Chemistry: X-Ray Diffraction Analysis; Wiley—Interscience: Chichester, 1980; p 488.
13. Leob, S.; Sourirajan, S. Adv Chem Ser 1962, 38, 117.
14. Reuvers, A. J.; Van den Berg, J. W. A.; Smolders, C. A. J Membr Sci 1987, 34(1), 45.
15. Reuvers, A. J.; Smolders, C. A. J Membr Sci 1987, 34(1), 67.